limit the availability of biopharmaceuticals to developing countries. Also the bioshield project (http://www.whitehouse.gov/infocus/bioshield/) proposes a longer shelf life (~10 years) for "next-generation" drugs including vaccines. In order to meet these requirements, strategies other than the traditional formulation methods are desired to further improve the stability of biopharmaceuticals.

Recently, it was reported that the stability of amorphous solids is also dependent on the process used to prepare the material, with "thermal history" being one critical factor.[5–7] Thus, the drying processes with different thermal histories may impact the stability of pharmaceuticals.[8,9] Glass dynamics have been proposed as an important factor in the stabilization effect of amorphous excipients on proteins during drying and storage[10,11] This mechanism states that the excipient forms a rigid matrix in which the protein is molecularly dispersed, and the limited mobility in the high viscosity glass slows down the protein mobility which is necessary for protein degradation. According to the Stokes–Einstein equation, the diffusion coefficient in supercooled liquid is inversely proportional to the viscosity of the system.[12] Structural relaxation time, a measure of molecular mobility, is also related to the diffusion coefficient.[11,12] Thus, chemical reactions that require diffusion can have a dependence on molecular mobility or structural relaxation time of the system.

DSC and other calorimetry studies suggest that a correlation does exist between chemical instability and the structural relaxation time of the amorphous system.[13–19] For example, Duddu et al.[17] reported the correlation of aggregation of an IgG1 antibody with the reduced time (t/τ) below T_g. Shamblin et al.[18] reported strong coupling between the dimerization rate of ethacrynate sodium (ECA) and structural relaxation time in formulations cofyophilized with sucrose, trehalose, and PVP. Recently, it was found that there is a correlation between the rate of degradation and structural relaxation time in human growth hormone (hGH) protein systems lyophilized with several sugars.[19] However, it is also noticed that there are reports in pharmaceutical literature that provide examples of a poor correlation. The contribution of molecular mobility was found to be small in insulin degradation in trehalose formulations under high humidity conditions,[20] as well as with PVP.[21] Therefore, while there are numerous examples of a correlation between structural relaxation and reactivity, the correlations may not always be strong.

Thermal treatment of dried glass results in an increase in the structural relaxation time (or decrease in global mobility). A glass is in a nonequilibrium state and it exhibits higher enthalpy, free energy, and entropy than the corresponding equilibrium supercooled liquid. Due to its higher energy, a glass will relax toward the equilibrium curve in an experimentally accessible timescale if there is sufficient mobility. The process of relaxation toward equilibrium is known as physical aging or annealing.[22] In this article, we use "annealing" to describe a process wherein an amorphous material is kept at a temperature below T_g for a period of time sufficient to allow significant relaxation toward the equilibrium state. During the annealing period, some physical and mechanical properties of amorphous solid will change with time. For example, the time-dependent changes in glassy polymers upon annealing include increase in density, yield stress, and decreases in stress relaxation rate, free volume, and enthalpy.[22,23] For our interests, the primary effect of annealing of amorphous glass is the increase in structural relaxation times and thus reduction in global mobility.[8,22,23]

If chemical/physical stability and structural relaxation time are coupled in a glass, then a sample with a larger structural relaxation time resulting from annealing should have better stability. That is, stabilization against pharmaceutical degradation could be achieved by annealing for a short period of time. There are several studies supporting the concept of "stabilization by annealing" in both the food and the pharmaceutical literature. The first demonstrated example of stabilization of pharmaceuticals by annealing involved an antibacterial (moxalactam disodium) formulation cofyophilized with 12% (w/w) mannitol.[24] Drying of the antibacterial system (with a T_g about 121°C) using 60°C instead of 40°C during the secondary drying process gave samples of essentially identical residual moisture but the higher temperature drying protocol gave a systematic improvement in storage stability that averages about 20%. This system was further investigated, and the stabilization effect was correlated to the reduced molecular mobility.[25] Hill et al.[5] studied the annealing effect in food systems, and the rate of Maillard reaction between lysine and glucose was found to be about 20% slower in the aged glassy matrix after aging for 3 weeks at a temperature of 30°C below T_g.

DOI 10.1002/jps

Luthra et al.[25] reported that rate of cyclization degradation reaction in aspartame/disaccharide glass decreases significantly when the freeze-dried sample was heat treated postlyophilization in an oven. Recently, it was found that annealing resulted in the decrease in dimerization rate of ECA, and thus annealing can also stabilize intermolecular degradation reactions that involves mobility on longer length scales such as dimerization processes.[27] While these observations show that thermal treatment may be used to increase the long-term stability, evidence for this stabilization effect on amorphous pharmaceuticals is still limited. Furthermore, these annealing studies only focused on small molecule pharmaceuticals, and the consequence of annealing on delicate large protein molecules is unknown. Given the desire to improve the stability of biologics, it will be very important to determine if protein biopharmaceuticals can also be stabilized by annealing.

In this article, the impact of annealing on the stability of an IgG1 fusion protein is investigated. Previous studies showed that the stabilization effect from sugar is dependent on the disaccharide level, and a formulation with higher sucrose level generally exhibited much better storage stability.[19,28,29] However, a protein formulation with higher sugar level is not always practical due to limits imposed by the disease state (such as diabetes) or manufacturing constraints (such as long lyophilization cycle due to high solid content associated with high sucrose level). Here, low sugar content formulations would be preferred if sufficient stability can be obtained, for example, by annealing. We have chosen two formulations with low-to-moderate sugar level (sucrose/IgG1 protein mass ratio of 0.5 and 1) in this study and have conducted an extensive investigation of the impact of annealing on selected physical properties, protein structure in the solid, molecular mobility, and aggregation stability.

EXPERIMENTAL

Materials

A recombinant humanized IgG1 fusion protein with a molecular weight of 185 kDa was provided by Wyeth Biopharma (Andover, MA). The protein drug substance was ultrafiltered through a regenerated cellulose membrane filter (Billerica, MA, area of 50 cm^2, 30 kDa molecular weight cutoff value).[1] The L-histidine, sodium chloride, poly-L-lysine, 2-hydroxylpropyl-β-cyclodextrin, pluronic F68 (a hydrophilic nonionic surfactant), polysorbate-80, and glycine were purchased from Sigma (St. Louis, MO). D-Sucrose with reduced heavy metal (<5 ppm) content was purchased from Calbiochem of EMD Biosciences (San Diego, CA). These reagents were of the highest grade available and were used without further purification.

Lyophilization Procedures

Ten milligrams per milliliter IgG1 protein solutions were prepared after dialysis against two buffer solutions: one buffer was 1 mM histidine buffer (pH 6.5), and another was 1 mM histidine buffer and 40 mg/mL of sucrose (pH 6.5). By mixing two stock solutions at different ratios, two protein formulations with sucrose/IgG1 protein mass ratios of 0.5 and 1 were prepared. The formulation with sucrose/IgG1 protein mass ratios of 0.5 and 1 is defined as P10S5 and P10S10, respectively, where P represents the protein, S represents sucrose, and the number is the concentration (mg/mL) of the component in the formulation.

Protein solutions (1 mL) were filled into 2 mL tubing glass vials and were lyophilized in a Genesis 25 EL (SP Industries, Gardiner, NY) freeze-dryer. The samples were first dried at a shelf temperature of −25°C with a chamber pressure of 6.6 Pa (50 mT) for 30 h, and then the samples were further dried at about 4 Pa (30 mT) with a shelf temperature of −25°C for 35 h. Primary drying was conducted below the glass transition temperature of freeze-concentrate (T_g') of both formulations. Secondary drying was carried out for 6 h at 25°C. After the drying process was finished, vials were stoppered under dry nitrogen with Daikyo Flurotec stoppers (West Pharmaceutical, Lititz, PA) and capped with aluminum seals. All the samples were amorphous after freeze-drying as evidenced by the absence of birefringence with polarized light microscopy (PLM; Linkam, McCrone, Chicago, IL).

Residual Water Measurement

The water content for each formulation after freeze-drying was determined using Metrohm

[1] Certain commercial equipment and materials are identified to specify adequately the experimental procedure. In no case does such identification imply recommendation by the National Institute of Standards and Technology, nor does it imply that the material or equipment identified is necessarily the best available for this purpose.

Karl Fischer coulometer (Riverview, FL). At least two vials of each sample were used. Freeze-dried sample vials were reconstituted in 2 mL dried methanol and 0.5 mL of the solution was injected into the titrator. Blank corrections were applied. Standard deviation from replicate measurements was less than 0.2% (w/w).

Specific Surface Area Measurement

Specific surface area (SSA) analysis was performed using a FlowSorb II 2300 surface area analyzer (Micromeritics, Norcross, GA). A protein sample of about 100 mg was loaded into the sample holder in the glove bag with controlled humidity (<2%). Single point calibration was performed prior to taking surface area measurements using 1 mL Krypton gas. Powder samples were degassed for at least 3 h at 35°C in the Flow Prep oven, and surface areas were measured using krypton (Kr) as an adsorbate and helium as carrier.

Differential Scanning Calorimeter (DSC) Measurements

Modulated DSC (Q1000; TA Instruments, New Castle, DE) was used to measure the glass transition temperature (T_g) and the change in heat capacity at T_g (ΔC_p) of protein samples. The samples were run at a 2°C/min heating rate, modulated with a ±1°C amplitude every 120 s. Fresh protein samples with sucrose/protein mass ratios of 0.5 and 1 give T_g of 106 and 101°C (mid-points), respectively.

Enthalpy recovery (ΔH) of the annealed sample was measured using standard (nonmodulated) DSC following the previously described procedure.[27] The scan rate used was 10°C/min. Briefly, the heating curve of the first DSC scan was used to obtain the area of the endothermic recovery peak by integration using Universal Analysis Software (TA Instruments). The thermal history of the annealed sample was then erased by holding the sample at a temperature above T_g, the sample was cooled, and a second DSC curve was obtained, representing zero annealing time. The second scan curve is given in Figure 1. We define the enthalpy recovery (ΔH) as the enthalpy difference between the annealed sample and the sample with erased thermal history.

The relaxation enthalpy at infinite time (ΔH_∞) at a given annealing temperature (T_a) was

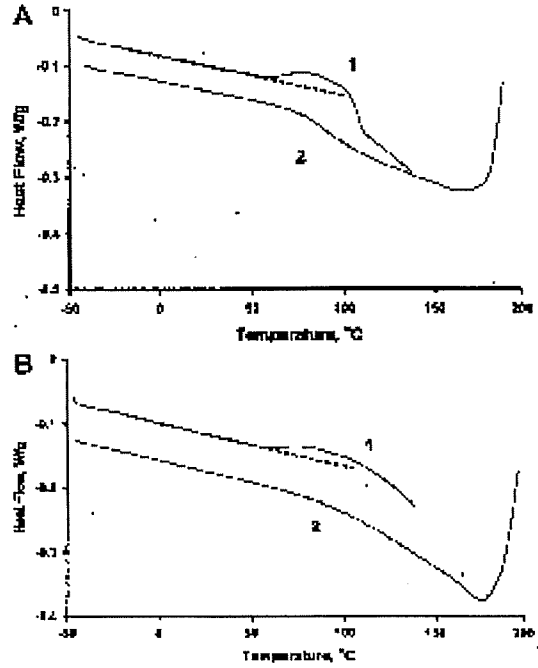

Figure 1. DSC of a fresh lgG1/sucrose sample showing the endothermic pre-T_g peak in the P10S10 formulation (A) and P10S6 formulation (B). The dashed line in the first scan (curve 1) is added to guide the eye to differentiate the pre-T_g event. The second scan after eliminating the thermal history (curve 2) showed the disappearance of pre-T_g event. The lines were offset for clarity.

calculated using the following equation:[30,31]

$$\Delta H_\infty = (T_g - T_a) \times \Delta C_p \quad (1)$$

A relaxation function (Φ) served as a measure of the extent of enthalpy relaxation during annealing and was calculated as follows:[31–35]

$$\Phi = 1 - \frac{\Delta H}{\Delta H_\infty} \quad (2)$$

where ΔH is the enthalpy recovery measured from DSC and ΔH_∞ is the corresponding value at time infinity as obtained from Eq. (1).

Structural Relaxation Time Measurement by Thermal Activity Monitor

Isothermal microcalorimetry was used to measure the rate of enthalpy relaxation of the sample at the storage temperature (50°C) using a Thermometric, 2277 Thermal Activity Monitor (Thermo-

DOI 10.1002/jps

metric, Jarfalla, Sweden). The experimental procedure and data analysis using Kohlrausch–Williams–Watts (KWW) curve fitting is similar to that described in a previous report.[37]

Studies of Protein Aggregation by Size Exclusion Chromatogram

Assay for chemical degradation was not routinely performed because the protein samples did not show sufficient chemical degradation to allow a quantitative analysis of chemical instability. Size exclusion chromatography (SE-HPLC) was used to assess the physical aggregation of the protein during storage. The initial SE-HPLC assays were run on both fresh samples (nonannealed) and on samples exposed to different annealing conditions. The rest of the sample vials were then transferred to an oven at 50°C. After storing for preset times (0.5, 1, 3, and 6 months), the samples were reconstituted with 1 mL of purified water. All solutions obtained were visually clear after reconstitution, and the soluble protein aggregate was analyzed with HPLC.

A column of YMC DL20S05-3000WT (Waters, Milford, MA) was used with a flow rate of 1 mL/min. The mobile phase consisted of 0.05 mol/L NaH_2PO_4 and 0.2 mol/L NaCl (pH 7.2). UV absorption was monitored at 280 nm. The dimer eluted at about 6.2 min and the monomer peak appeared at about 6.8 min. The standard error in the percentage of aggregate for all sample replicates was <0.5%.

To evaluate the effect of variable diluent composition on the measured aggregation, reconstitution of lyophilized protein formulations was also carried out using reconstitution media containing 0.5% (w/w) additives such as phosphate buffer, dextran sulfate, 2-hydroxylpropyl-β-cyclodextrin, pluronic F-68, and polysorbate-80. Then, the amount of aggregate in the reconstituted sample was measured by SE-HPLC analysis.

Protein Structure Characterization by FTIR

Fourier transform infrared spectroscopy (FTIR) studies were conducted using a Nicolet Magna-IR 560 spectrometer (Thermo Electron, Madison, WI). The study was carried out using transmission mode on the freeze-dried protein solids according to procedures in the literature.[34,35] A total of 128 scans and 4 cm^{-1} resolution were used for each spectrum. About 2 mg of solid protein sample was mixed with 200 mg dried KBr powder, and the mixtures were then pressed with a Carver press at 11,000 psi for about 2 min. The obtained transparent pellet was put into the sample holder and then loaded into a dried air-purged measurement chamber. The protein spectrum was collected and the absorbance signal was obtained using the corresponding background. Second derivative spectra were then obtained using an OMNIC software. The second derivative of the amide I region (1700–1600 cm^{-1}) of the spectra was baseline corrected and area normalized. The peak height of the major band was used to compare the similarity between spectra.

Fast Local Dynamics from a Neutron Backscattering Spectrometer

The fast local dynamics with timescale of nanoseconds was studied with a high flux backscattering (HFBS) spectrometer at the Center for Neutron Research on the NG2 beam line at the National Institute of Standards and Technology (NIST).[38] Only those motions with timescales shorter than 5 ns can be measured with this instrument.[37] The details of the experimental procedure and data analysis have been published elsewhere.[37,38,39] A larger mean square of displacement of H-atom (msd, $\langle u^2 \rangle$) means a higher local mobility of the system.

Determination of $T_{1\rho}$ of Protein and Sucrose by ^{13}C Solid-State NMR

The rotating-frame spin-lattice relaxation time ($T_{1\rho}$) of the IgG1 carbonyl carbon in lyophilized protein/sucrose formulations was determined at 25°C using a UNITY plus spectrometer (Varian, Inc., Paulo Alto, CA) operating at a proton resonance frequency of 400 MHz. Spin-locking field was equivalent to 19 kHz. The rotor size was 7 mm and spinning speed was 4 kHz. Peak height at about 180 ppm due to IgG1 carbonyl carbon and 90 ppm from sucrose were followed with different delay times.[40] Similar measurement of $T_{1\rho}$ was performed for annealed protein samples. The data were fit to a biexponential decay model to determine the two $T_{1\rho}$ as reported elsewhere for freeze-dried systems.[39,41] Since the shorter $T_{1\rho}$ value was the same for all samples, the longer $T_{1\rho}$ values were used for comparison between samples annealed at different conditions.

RESULTS AND DISCUSSIONS

Impact of Annealing on Physical Properties of IgG1 Protein Samples

Annealing appeared to have no impact on the physical form or the SSA of the protein samples we studied. The fresh unannealed and annealed samples were confirmed to be amorphous by PLM. Even upon storage at 60°C for 6 months, we observed no crystallization of sucrose by PLM. Sample SSA was also unaffected by annealing. For the fresh unannealed sample, the SSA was approximately $1.7 \pm 0.2\ m^2/g$, which is similar to that reported for other protein pharmaceuticals.[6,42] After annealing at 70°C for 20 h, the most aggressive annealing protocol we used, the SSA of the aged sample was essentially unchanged at $1.9 \pm 0.1\ m^2/g$. This result was consistent with previous reports that aging did not lead to perceptible changes in morphology or particle size in a trehalose system.[43]

The impact of annealing on residual moisture of the protein sample was determined with Karl Fischer titration (Tab. 1). The fresh protein sample immediately after freeze drying showed low moisture level (about 0.5%, w/w). Upon annealing of protein samples at high temperatures for 10 or 20 h, the residual water increased by 0.5–1%. In addition, upon storage at 50°C for 3 months, all samples, fresh and annealed, showed a moisture level of about 2% (w/w). The increase in the moisture upon annealing or storage is believed due to the transfer of moisture from the stopper to the dried cake.[44–46] Even though there are changes in moisture during annealing, these small changes are not expected to significantly impact enthalpy relaxation and stability. In similar protein systems, changes in moisture from 0% to 3% showed only very slight changes in stability.[47] Also in previous peptide/sugar and ECA/sugar systems where there were large total sample amounts in a vial, no obvious changes in moisture were observed upon annealing, even though annealing caused significant changes in enthalpy relaxation.[25,27] In short, there is significant precedent for annealing causing increases in relaxation time and stabilization, even if not in protein systems, so the results obtained in this study are consistent with previous results. In addition, we note that the structural relaxation time increases sharply upon annealing as shown below from the TAM experiments, so the water plasticization effect on global molecular mobility is obviously overwhelmed by the annealing effect itself, so the impact of water content variations such as those shown in Table 1 on relaxation dynamics and stability is not expected to be significant.

Table 1. Percent Residual Water Content (%) in P1055 Sample upon Annealing at Different Conditions

Sample	Initial Sample (T_0)	Stored at 60°C for 3 Months
Fresh	0.5 ± 0.06	2.0 ± 0.2
An60d10h	1.0 ± 0.06	2.4 ± 0.2
An60d20h	1.0 ± 0.31	n/d
An70d10h	1.4 ± 0.06	2.3 ± 0.08
An70d20h	1.6 ± 0.32	n/d
An80d10h	1.4 ± 0.07	2.4 ± 0.16

n/d, not determined.
Standard error shown is based on three replicates. The term "An60d10h" means that the sample was annealed at 60°C for 10 h.

DSC Investigation of Pre-T_g Event and Enthalpy Recovery

Pre-T_g exothermic events have been reported for freshly freeze-dried glasses;[27,46–50] and here we investigated this phenomenon by DSC. The IgG1/sucrose formulations were scanned from about −50°C to a temperature above T_g. Figure 1 shows the DSC curves of fresh P10S10 (T_g of 101°C) and P10S5 (T_g of 106°C) formulations, which were dried for 6 h at 25°C in secondary drying. Notice that pre-T_g exothermic peaks were observed at about 60°C in both protein formulations in the first scan. To investigate the source of the pre-T_g peak in the fresh sample, the DSC sample was kept at a temperature of about 30°C above T_g for 5 min to erase the thermal history of the glass, and then cooled down to −50°C and rescanned. The second scan showed a typical glass transition, with a clear absence of a pre-T_g exothermic peak in both formulations.[48,50] This suggests that the pre-T_g event in the freshly lyophilized sample is a result of the thermal history it experienced during the normal freeze-drying cycle.

The pre-T_g event in annealed protein samples was also investigated using DSC. The impact of annealing on DSC behaviors of P10S10 and P10S5 is shown in Figure 2. Upon annealing at low temperature, the pre-T_g exothermic peak converted to pre-T_g endothermic peak for both samples. Increasing the annealing temperature resulted

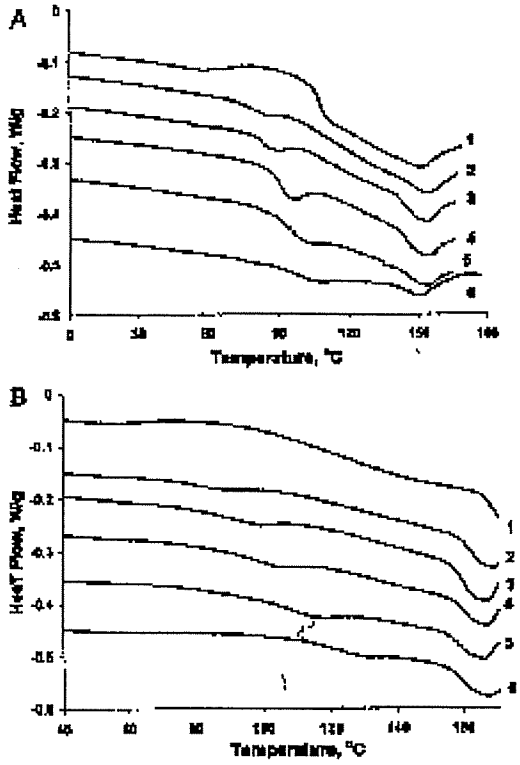

Figure 2. DSC curves of unannealed fresh IgG1/sucrose sample (curve 1) and samples annealed for 20 h at different temperatures. (A) P10S10 formulation annealed at 60°C (curve 2), 65°C (curve 3), 75°C (curve 4), 85°C (curve 5), and 90°C (curve 6). (B) P10S5 formulations annealed at 60°C (curve 2), 70°C (curve 3), 80°C (curve 4), 90°C (curve 5), and 105°C (curve 6). The endothermic thermal events around 150°C (P10S10) and 170°C (P10S5) are likely denaturation endotherms while the thermal events at lower temperatures represent T_g and relaxation events.

in the shift of the endothermic peak to a higher temperature, and finally the peak appeared as a T_g overshoot. The physical basis of the pre-T_g events is not well understood even though these events have been reported elsewhere.[47,48,61,63] Our studies show that annealing significantly impacts pre-T_g events, but as discussed below, we observe no impact of annealing on β relaxation, either as measured by neutron scattering or by NMR. Thus, it seems that pre-T_g event is not a result of β relaxation motions. Presumably these peaks are associated with a very broad distribution of the structural relaxing populations.[8,48,59–62,64] It is possible that some relaxing species may have relaxation times shorter than the annealing time at the annealing temperature, and thus they have relaxed during the annealing step.[46] Upon reheating the sample during the DSC scan, these fast relaxing species may regain the lost energy which then results in the formation of a pre-T_g endotherm.[37]

The enthalpy relaxation upon annealing was studied as a function of annealing time and temperature. For relaxation studies using DSC, it is assumed that the enthalpy relaxation that occurred during the annealing process is identical to the enthalpy recovery measured during the heating scan in DSC. Here, enthalpy recovery was determined by integration of the endothermic peak with a sigmoidal baseline feature, as discussed in the Experimental Section. Figure 3 shows the impact of annealing temperature on the enthalpy recovery of IgG1/sucrose formulations. The magnitude of enthalpy recovery increased upon increasing the aging temperature initially. However, a maximum enthalpy recovery was observed at about 85°C for the P10S10 formulation, and further increases in annealing temperature produced a decrease in the enthalpy recovery. Similarly, a maximum enthalpy recovery is observed at about 90°C for the P10S5 formulation. Thus, both formulations give a maximum

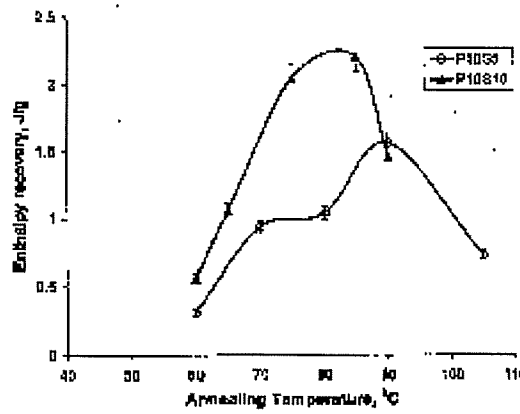

Figure 3. Impact of annealing temperature on the enthalpy recovery of IgG1/sucrose formulations after annealing for 20 h. Note the enthalpy recovery reaches a maximum for both protein formulations at about 15°C below T_g. Error bars are standard errors for 2–3 replicates.

enthalpy recovery at about 15°C below their T_g, which is expected based on previous studies [27,46]

The impact of annealing time on enthalpy recovery was also investigated. The enthalpy recovery was found to be proportional to the log of annealing time (results not shown), which is consistent with previous report on small pharmaceutical molecules.[26,27] The logarithmic dependence of enthalpy on annealing time means that the enthalpy relaxes much more rapidly in the short time range than at longer times. Density studies from this laboratory (unpublished) on the pure trehalose system also showed that the density increase (or free volume decrease) is most pronounced early in the annealing process (for about 5–10 h). Thus, for the application of annealing to lyophilization cycle development, the annealing time has been selected to be 10 or 20 h in our study.

Figure 3 shows that P10S10 give larger enthalpy recovery than P10S5 upon annealing at the same conditions (60°C for 20 h). Also the P10S10 sample annealed at 75°C exhibited higher enthalpy recovery than the P10S5 sample annealed at 60°C for the same periods of time. Therefore, it seems that the protein formulation with higher sucrose fraction shows higher enthalpy recovery than the protein formulation with lower sucrose level. This observation is a direct result of Eq. (1) and the larger ΔC_p for a system richer in sucrose. As a strong glass, a pure protein exhibits a very broad T_g with a very small heat capacity change, ΔC_p, which makes it difficult or impossible to measure the T_g of pure proteins with DSC.[50] In contrast, sucrose is a fragile glass and exhibits large ΔC_p at T_g, and thus the enthalpy relaxation in sucrose is much larger than in a protein according to Eq. (1).

Investigation of the Impact of Annealing on the Storage Stability of IgG1

In order to determine if the reconstitution process will impact the measured aggregation, the effect of reconstitution media on the amount of protein aggregate measured was studied. Table 2 shows the aggregate level in the IgG1 protein formulation upon reconstitution in fresh and annealed samples. We note that the addition of surfactant or polyanions did not significantly impact the amount of aggregation measured. Similar observations have been made for some other proteins.[39,40] Thus, for the systems studied in this research, the reconstitution process did not significantly impact aggregate formation. We thus conclude that stability differences of the IgG1 protein upon annealing are mainly the result of the bimolecular aggregation events that actually occur in the solid-state during storage. That is, development of aggregation that correlates with storage time and conditions could reflect a bimolecular aggregation event that occurs during storage or could reflect time-dependent protein structural alteration during storage, with the actual aggregation event occurring mostly during reconstitution when molecular mobility becomes very high. For our systems, the role of aggregation during reconstitution is, at best, minimal.

The time dependence of IgG1 aggregation upon storage at 50°C was studied for both protein formulations. As shown in Figure 4A, the fresh sample of the P10S10 formulation showed less degradation than the annealed sample at time 0, as expected because some degradation will occur during annealing. However, upon storage for about 1 month, these samples showed almost identical aggregate level, and further storage for

Table 2. Effects of Reconstitution Medium on the Amount of Protein Aggregation Measured in the P10S5 Formulation upon Lyophilization and Storage at 50°C

Reconstitution Medium	Immediately After Freeze Drying	Anneal at 50°C for 7 Days
Water	5.5 (0.32)	6.8 (0.17)
Phosphate buffer	5.6 (0.27)	9.0 (0.14)
Dextran sulfate	5.8 (0.14)	9.1 (0.18)
2-hydroxylpropyl-β-cyclodextrin	5.8 (0.16)	8.9 (0.04)
Pluronic F-68	5.5 (0.18)	8.8 (0.12)
Tween-80	5.3 (0.20)	8.7 (0.11)

0% additives unless specified otherwise
Values in brackets represent standard deviation ($n = 6$).

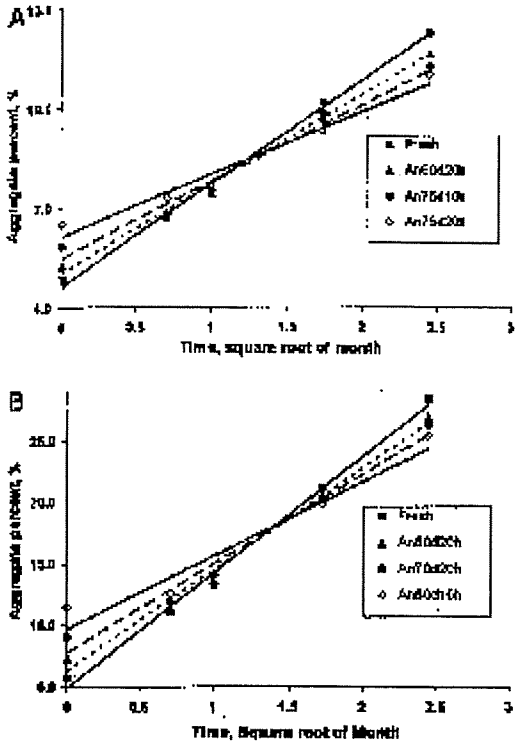

Figure 4. Time dependence of IgG2 aggregation upon storage at 50°C for P10S10 (A) and P10S5 formulation (B). Note the linear relationship between the protein aggregation and square root of time in the x-axis. The correlation coefficients for P10S10 are 0.996, 0.991, 0.987, and 0.968 with increasing annealing temperature. The regression coefficient for P10S5 is 0.993, 0.989, 0.979, and 0.937 with increasing annealing temperature. The slope of the best-fit straight line is used as the degradation rate constant. The error bars are about the size of the symbol.

longer times resulted in the annealed sample having less aggregation. That is, the annealed sample not only showed a lower degradation rate during storage (i.e., smaller slope), but in spite of the degradation suffered during annealing, actually exhibited less total degradation at the end of storage than the fresh sample. These data (Fig. 4A) are an excellent example of large differences in stability that can result from annealing. Similar to the P10S10 formulation, annealing also stabilizes the protein-rich P10S5 formulation as shown in Figure 4B. Again, annealed samples exhibited lower total aggregate levels after storage for more than about 2 months. Thus, our postulate that protein systems can be stabilized by annealing is valid for both IgG1 formulations.

The protein aggregation kinetics in freeze-dried solids were evaluated and these stability data were found to fit square root of time model best, as measured by a high correlation coefficient.[27] The correlation coefficients, as shown in Figure 4, are still relatively high enough even though they do seem to decrease upon increasing annealing temperature. Since the fit to square root of time model was better than the first-order kinetics even for the annealed samples, the square root of kinetics was used throughout the article for consistency when comparing the storage stability of different samples. This square root of time degradation kinetics is commonly observed in glassy materials.[19,25–27,81,83] Therefore, the aggregation rate constants were obtained as the slope of the straight line in Figure 4. Table 3 shows the aggregation rate constants and initial aggregate levels of IgG1 protein at 50°C upon annealing at different conditions. The annealed P10S10 formulation had only slightly higher initial degradation in the annealed samples relative to the unannealed system (with initial aggregate range from 4.8% in fresh to 6.5% maximum in annealed), which is due to degradation occurring during the thermal treatment. In contrast, the P10S5 formulation gives a relatively large change in initial aggregate upon annealing at high temperature. Also, the P10S5 formulation gave a higher rate of degradation as compared to the P10S10 formulation with the same thermal history. The better stability in P10S10 than P10S5 is consistent with previous findings that a higher amount of sucrose in protein formulations can afford better protection to the protein in the glassy solid.[19,38,82] It was found that P10S10 formulation showed lower molecular mobility, lower free volume, and lower degree of native structure perturbation than P10S5,[39] all of which are consistent with the better stability in P10S10 than P10S5 upon annealing and storage.

The general trend in the physical stability data shows that as annealing temperature increased, long-term stability improved (i.e., the rate constant decreased). Therefore, annealing below T_g can slow down the aggregation rate of the protein. In spite of increased initial aggregation after the annealing process, annealed samples actually showed less aggregation after storage for 3 and 6 months (see Fig. 4). For P10S10, the control

Table 3. Initial Aggregation Level and Aggregation Rate Constants of IgG1 Protein Sucrose Formulations at 50°C upon Annealing at Different Conditions

Annealing Temperature (°C)	Annealing Time (h)	Initial % Aggregation	k at 50°C
P10 S10 control (fresh)		4.8 ± 0.1	3.1 ± 0.1
60	10	5.1 ± 0.1	2.9 ± 0.1
60	20	5.3 ± 0.2	2.7 ± 0.1
65	10	5.4 ± 0.3	2.8 ± 0.2
65	20	5.6 ± 0.4	2.6 ± 0.2
75	10	5.8 ± 0.3	2.3 ± 0.2
75	20	6.5 ± 0.3	1.9 ± 0.2
P10 S5 control (fresh)		5.8 ± 0.2	9.4 ± 0.6
60	10	6.9 ± 0.3	5.8 ± 0.6
60	20	7.4 ± 0.3	5.2 ± 0.6
70	10	7.9 ± 0.4	7.6 ± 0.4
70	20	9.1 ± 0.3	7.2 ± 0.6
80	10	11.6 ± 0.3	6.0 ± 0.8
80	20	13.3 ± 0.4	5.6 ± 0.6

Uncertainties given for the rate constants are standard errors as provided by the regression analysis based on the square root of time kinetics.

(fresh) sample and sample annealed at 75°C for 20 h give degradation rate constants of 3.1 and 1.9, respectively. Thus, annealing results in a decrease in degradation rate constant of about 40% for IgG1 protein. Also the P10S5 sample annealed at 60°C gives similar improvement in stability. These data (Tab. 3 and Fig. 4) clearly demonstrate that annealing improves long-term stability of the IgG1 protein.

In order to further address the question "Does annealing significantly impact aggregation of IgG1 protein?," a statistical test using the general linear model (GLM) procedure was performed on the rate constant data to determine the effect of both annealing temperature and time. The GLM results for P10S5 data showed a significant contribution of both annealing time ($p = 0.068$) and annealing temperature ($p < 0.001$) on the differences observed in aggregation rate between control (fresh) and annealed samples. Similarly, annealing significantly improved the stability of the P10S10 sample. Therefore, both annealing time and temperature significantly impact the stability.[27] It should be pointed out that initial degradation level may need to be considered to address product quality in a broader sense, as, for example, if there is potential toxicity and/or immunogenicity due to the degradation product produced during annealing. In the current study, the initial aggregate level upon annealing is relatively high due to the protein drug substance, formulations, and annealing conditions used, but it should be emphasized that the total aggregate level of the annealed sample is less than that for the nonannealed sample after about 2 months into the stability study. Moreover, the amount of degradation during annealing is protein, formulation, and process dependent. For example, our unpublished results on rHSA systems showed that the initial aggregate upon thermal treatment at 65°C for 30 h was still <0.5%, and a similar stabilization effect was observed upon annealing. In this example, the annealing approach is obviously a practical procedure for improving stability.

Impact of Annealing on Protein Native Structure

Figure 5 shows the impact of annealing on the protein structure in the solid as determined by area-normalized FTIR spectra of the IgG1 formulations. The spectra are characteristic of IgG1 protein which has a predominance of β-sheet structure at 1641 and 1693 cm^{-1}. Figure 5 shows the FTIR spectra of P10S10 after annealing at 70°C for different periods of time. After annealing at 70°C for 10 h, the peak height at 1641 cm^{-1} was essentially the same as the fresh sample. Even a sample annealed at 70°C for up to 40 h showed no

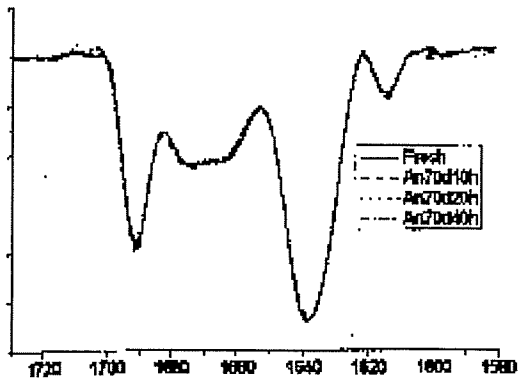

Figure 5. Area-normalized second derivative FTIR spectra of IgG1 P10S10 formulations after annealing at different conditions. Notice that no significant change in protein structure was observed upon high-temperature annealing. The data in the curve represent the average of three replicates.

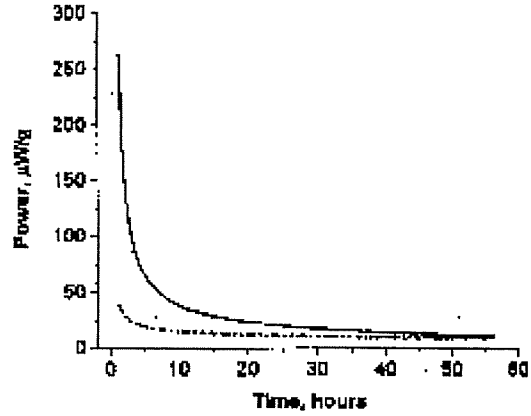

Figure 6. Power-time data at 50°C for a P10S10 sample annealed at 75°C for 10 h (dashed line) and fresh control sample (solid line). Note the higher power in the fresh sample than the annealed sample at same time, which indicates that annealed sample has a much lower molecular mobility.

obvious change in the amide I band. The same qualitative result has been observed for the P10S5 formulation (data not shown). These results indicate that no significant differences in the secondary structure of the protein are produced upon annealing for either formulation, at least within the sensitivity of the technique. The tertiary structure of the IgG1 upon reconstitution was also studied using fluorescence spectroscopy, and it was found that there was no significant shift in the emission peak maximum for both tyrosine and tryptophan residues upon annealing of P10S10 at 65°C for 10 h (data not shown). Of course, this does not mean changes in tertiary structure did not exist in the solid but simply "refolded" upon reconstitution. Since methodology suitable for characterization of tertiary structure in the glassy is not available, we studied secondary structure by FTIR. As indicated above, no changes in secondary structure upon annealing were observed. These results are consistent with recent observation that thermal denaturation of hGH in a glassy solid occurs only well above T_g.[55] FTIR, HPLC, and DSC results indicated that brief exposure of hGH to temperatures slightly less than the onset denaturation temperature in dried solid (i.e., below 150°C) did not cause significant damage to the protein.[63] These results suggest that thermal treatment of dry solids at a temperature well below T_g does not cause significant change of protein native structure.

Impact of Annealing on the Global Mobility

The rate of enthalpy loss was monitored using isothermal microcalorimetry. Figure 6 compares the thermal activity versus time curves at 50°C for control and annealed P10S10 samples. The thermal activity of the both samples decreases rapidly in the first 10 h, and then decreases slowly. This relaxation behavior is normally observed and is due to structural heterogeneity in the system.[6,38] It is widely accepted that a glass consists of a collection of "substates" with different sizes and entropies, each relaxing independently at different rates, giving rise to a broad distribution of structural relaxation times.[38,61,65] Also note (Fig. 6) that the annealed protein sample shows a very small heat flow signal compared to the

Table 4. Structural Relaxation Time Constant (τ^β) of P10S10 Sample at 50°C With Different Thermal Histories

Annealing Temperature (°C)	Annealing Time (h)	
	10	20
Fresh control	2.3 ± 0.6	
60	42 ± 3	49 ± 9
65	48 ± 5	41 ± 5
75	45 ± 4	52 ± 6

The τ^β value was calculated based on fitting of TAM data to the KWW model. The uncertainty is the standard error based on 2–3 replicates.

unannealed control sample. The effect of annealing conditions on the structural relaxation parameters of P10S10 is shown in Table 4. All annealed samples showed a large decrease in molecular mobility, as shown by the large increase in t^β value from 2.3 for the control sample to about 40–50 after annealing. This decrease in global mobility upon annealing is caused by the post-lyophilization annealing process. The substates with small relaxation times are depopulated during annealing, leaving behind the populations with longer relaxation times. Therefore, annealing results in the increase in the relaxation time constant (i.e., a decrease in molecular mobility), as expected.

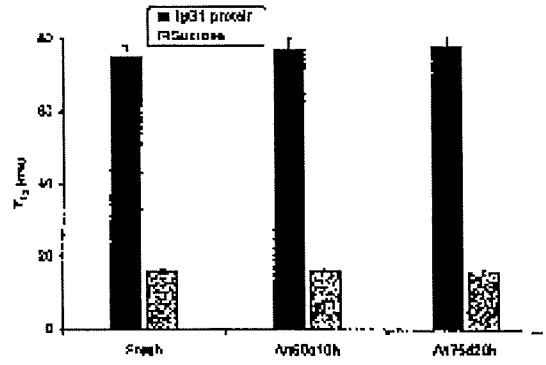

Figure 7. Impact of annealing on the rotating frame spin-lattice relaxation time ($T_{1\rho}$) of the IgG1 protein and sucrose matrix in the P10S10 formulation studied by solid state ^{13}C NMR at 25°C. Error bars represent the uncertainty from the best fit of data to the model.

Local Dynamics Measurement by Neutron Scattering and Solid-State NMR

The effects of annealing on local motions with timescales much shorter than global motions were also investigated. The fast local mobility with a timescale of <5 ns was investigated with neutron backscattering, and the mean-squared displacement ($\langle u^2 \rangle$) of the hydrogen atomic motion was recorded at temperatures ranging from 40 to 330 K. Table 5 shows the $\langle u^2 \rangle$ of the P10S10 samples with different thermal histories at 25, 40, and 50°C. $\langle u^2 \rangle$ values increase monotonically with temperature for both samples, which reflects the higher mobility of the sample at higher temperature. However, there is no significant difference in the $\langle u^2 \rangle$ of the control (fresh) sample and the sample annealed at 60°C for 10 h at any temperature studied. Thus, it seems that the annealing does not significantly impact the fast local mobility in the protein/sucrose system, at least for the annealing conditions studied. This finding is consistent with the previous neutron backscattering study on ECA system with ECA/sugar mass ratio of 1:10.[27] Even upon moderate to strong annealing of ECA/sugar formulations, no systematic differences in $\langle u^2 \rangle$ were observed for either ECA/sucrose and ECA/trehalose samples.

Table 5. Fast Local Mobility ($\langle u^2 \rangle$) of the P10S10 Sample Studied With Neutron Backscattering at Temperature of 25, 40, and 50°C

T (°C)	Fresh	An60d10h
50	0.297 ± 0.005	0.286 ± 0.006
40	0.284 ± 0.006	0.273 ± 0.005
25	0.264 ± 0.006	0.253 ± 0.005

Standard error shown is the uncertainty in the best fit of data to a Debye–Waller harmonic model.

The local molecular motion in the protein sample was also studied with high-resolution solid-state ^{13}C NMR. Due to the specificity of the technique, it is possible to separate the motions in the protein molecule at 180 ppm due to the IgG1 carbonyl carbon from motions of sucrose at 80 ppm. Figure 7 shows the spin-lattice relaxation times ($T_{1\rho}$) in the protein and the sucrose molecules upon annealing at different conditions. Annealing at 60°C for 10 h did not cause a significant change in $T_{1\rho}$ relaxation time in either protein or sucrose molecules. Strong annealing of the protein sample at 75°C for 20 h still did not produce an obvious change in relaxation time for either protein or sucrose molecules. Thus, it seems that even though the global molecular mobility was significantly impacted by these annealing conditions, the local dynamics studied by both neutron scattering and ^{13}C NMR were not affected by annealing in the IgG1 protein/sucrose system. Since motions monitored by neutron scattering and ^{13}C NMR have different time and length scales, these different techniques may detect different parts of the local motions in the system. Given the consistent results by both techniques, we conclude that, contrary to the impact of annealing on both global mobility (i.e., TAM measured) and stability, annealing does not significantly affect local motions of the protein system, at least for the annealing conditions investigated.

However, the impact of annealing on local mobility does seem to be variable, as documented in the literature.[41,56–63] Thus, the impact of physical aging on the local mobility (beta relaxation) may depend on the nature of the sample, aging conditions, and/or detection techniques.[24] Large protein molecules are quite different from small organic molecules in that they have unique internal protein motions such as partial unfolding transitions;[55,64] thus different motions may be measured in protein systems than in synthetic polymers or small molecule organic systems, even when using the same technique.

Correlation of Stability With Protein Structure and Molecular Mobility

FTIR structure of the protein does not change significantly upon annealing for either protein formulation. However, the long-term stability clearly increases upon annealing as shown by the decrease in the aggregation rate constant. Obviously, changes in protein secondary structure are not the origin of the improved stability upon annealing, and thus we look to changes in dynamics as the mechanism to account for the stability trends.

We note that, in our system, the protein stability does not correlate with glass transition temperature. It has been reported that the degradation rate of a pharmaceutical correlates with $T-T_g$, at least for several systems,[51,54] where formulation with a higher T_g may show better stability. However, T_g of the IgG2 protein formulations is not significantly impacted by the annealing, as noticed by DSC. Also the formulation of P10S10 gives much better stability than that of P10S5 even though P10S10 has a lower T_g that P10S5. Thus, a formulation with high T_g does not necessarily mean better stability, and $T-T_g$ is not a good predictor of protein stability, at least at temperature well below T_g.[5,25,29]

Figure 8 shows the correlation of stability of P10S10 with global mobility at different annealing temperatures. For 10 h annealing (Fig. 8A), the increase in the annealing temperature caused a decrease in the aggregation rate constant and the global mobility ($1/\tau^\beta$). Thus, the improved stability upon annealing correlates qualitatively with reduced global mobility. Also, in order to evaluate the suitability of using DSC to correlate with stability, the trend of the relaxation function (Φ) upon annealing, calculated using Eq. (2), is also given in the graph. It is noticed that the

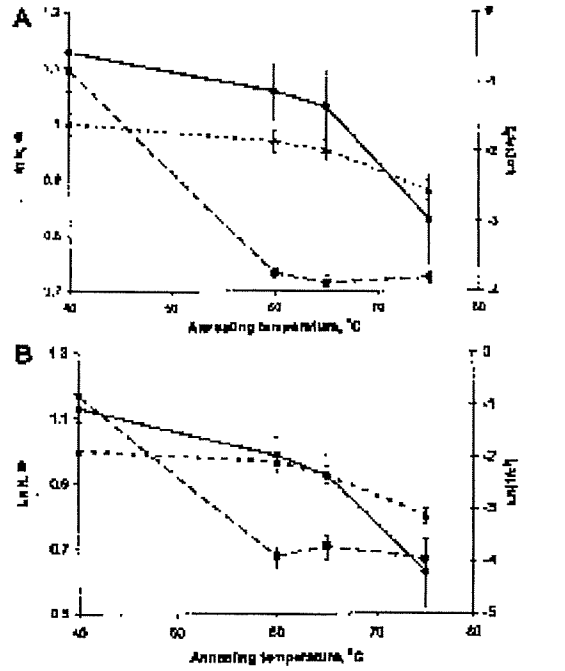

Figure 8. The relationship between physical stability (●, lnk_1), structural relaxation time(■, ln$[1/\tau^\beta]$), and initial relaxation function(Δ, Φ) for the P10S10 formulation after annealing for 10 h (A) and 20 h (B) at different temperatures. Error bars represent standard errors.

relaxation function decrease monotonically with increasing annealing temperature, which correlates with the decrease in the global mobility and aggregation rate constant. Therefore, similar to global mobility, the relaxation function obtained from a simple and fast DSC study may also be predictive of the protein stability. Further, the quantitative correlation with stability is better with Φ than with $1/\tau^\beta$. That is, the major change in $1/\tau^\beta$ occurs between the fresh sample and the sample annealed at 60°C, but for both the rate constant and Φ, the major change occurs between the samples annealed at 60 and 75°C. Figure 8B shows the same plot for the samples annealed at 20 h. Similar to 10 h annealing, the rate constant, global mobility, and relaxation function decrease with increase in the annealing temperature, but the quantitative correlation is best between stability and Φ. Figure 9 shows the correlation of aggregation rate constant with relaxation

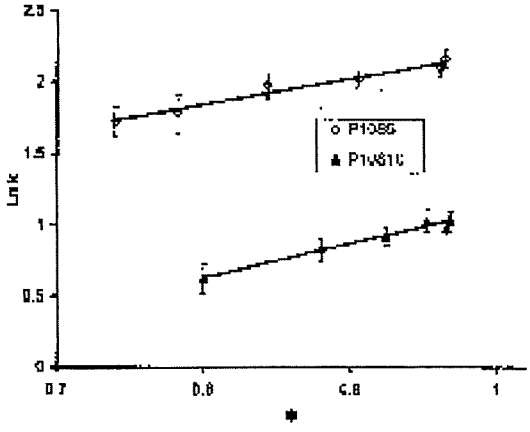

Figure 9. Correlation of protein aggregation rate with initial relaxation function (Φ) for both protein formulations. Error bar represents standard errors in the protein stability.

function for both protein formulations. Aggregation rate constants decreases with a decrease in relaxation function, showing an excellent linear correlation between ln(k) and Φ. Similar observations were made in a small molecule system (ECA/sugar system).[27] Therefore, it seems that the stability trend upon annealing may be well predicted using DSC data that is quick to obtain, uses little sample, and is quite precise relative to the structural relaxation time data obtained with isothermal calorimetry.

The better correlation of stability with Φ than with $1/\tau^{\beta}$ may be explained by the following factors. First, both TAM and DSC can be used to probe the enthalpy relaxation; however, these techniques may not measure exactly the same motion. It was found that the enthalpy relaxation obtained from the TAM was much higher than the enthalpy recovery obtained from DSC, which is consistent with previous observations that relaxation time constants obtained from DSC were larger than that from TAM for several systems.[65] This difference may be related to the much longer timescale for TAM experiment (several days) as compared to DSC experiment (minutes to hours), and it is possible that the TAM could measure some faster kinds of motion in addition to those motions related to enthalpy recovery (i.e., those that are mobilized only at or near the glass transition).[65] Second, it may be difficult to resolve small differences in τ^{β}, especially at a high annealing temperature. In the nonlinear curve fitting procedure for the calculation of τ^{β} using the KWW equation,[27,48] the fitting parameters have an uncertainty associated with both τ and β. The KWW equation assumes that the relaxation time is a constant. However, aging occurs during the calorimetric experiment, and τ constantly increases with time. The impact of this in-process aging on the values of τ and β has been studied,[31–33] and it was found that this experimental procedure often gave τ values much larger than the initial value of the sample but also gave β values that were too small. However, the structural relaxation time constant, τ^{β}, was found to be relatively constant and representative of the constant for the initial material (i.e., before the TAM run). Therefore, τ^{β} is usually considered a more reliable measure of global molecular mobility. However, this parameter is still subject to significant experimental error. The errors associated with τ in annealed protein formulations were about 10–15%, as given from the nonlinear regression analysis. The results reported in Table 4 are the average τ^{β} of 2–3 replicates, where the uncertainty shown (generally ~10–20%) reflects standard error of the mean from the replicates. We clearly do not have the accuracy to observe small differences in τ^{β}, especially at high annealing temperatures. All of the above factors may contribute to the different correlations of stability with $1/\tau^{\beta}$ and with Φ.

In the present study, an attempt has been made to address the question "What kind of mobility is relevant for stabilization: global, local or both?" It has previously been found that stability differences between protein formulations cannot be attributed solely to differences in global mobility,[13,35,37] and local mobility may also play an important role in protein stability. Recent studies on several proteins also showed that aggregation stability correlates well with local mobility but not with either global mobility or FTIR structure over the whole range of sucrose concentration studied (mass fraction range from 0 to 0.8).[39] Thus, fast, local motions may dominate the protein stability trends at temperatures well below T_g. In the present study, we find that annealing does not significantly impact the local dynamics of the protein formulation, as measured by either NMR or neutron backscattering, and this finding is consistent with previous observations with the small molecule ECA systems studied.[27] The results obtained here suggest that it is global mobility rather than either local

mobility or FTIR structure that correlates with the improved protein stability upon annealing. Thus, with due consideration of both previous observations and the results of this study, it seems that both global and local motion are relevant for protein stabilization, even though the relative importance of each kind of mobility for stabilization could vary depending on the system and experimental conditions such as temperature, and the variable being explored. The differences chemically and physically between the samples being investigated in a stability study of the effect of annealing do differ from differences typical of the samples in a stability study. Traditional stability studies focus on variations between different formulations that generally have large differences in chemical composition, glass transition temperature, fragility, and glass strength among the formulations. However, when annealing is the variable in a stability study, the chemical composition and T_g are constant, and variation in most physical properties is minimal. Although one might expect global mobility to dominate stability trends when differences in T_g and other bulk glass properties differ greatly, and local mobility to dominate stability trends when most bulk properties differ little, we actually observed the opposite behavior. When annealing is the stability variable, it seems that global mobility is the dominant factor for long-term stability.

CONCLUSIONS

This study demonstrated, for the first time, that drying process with different thermal histories (i.e., annealing) can have a significant impact on protein stability, and thus the details of the drying process need to be defined to control product stability. Moreover, the effect of thermal history on stability may be used to further stabilize fragile protein therapeutics through the use of appropriate annealing protocols. Annealing below T_g stabilized IgG1 protein formulations by decreasing the degradation rate such that not only was the degradation rate decreased by annealing but also the annealed sample actually exhibited lower total aggregation than the control (fresh) sample after a short storage time. Thus, the concept of "stabilization by annealing" is valid for the IgG1 protein system. Annealing does not significantly impact many properties, including the SSA, protein native structure, and local mobility; however, the enthalpy recovery and structural relaxation time constant increase upon annealing, and the improved stability upon thermal treatment is quantitatively correlated to the magnitude of relaxation function, and thus simple DSC studies may be used to guide the optimization of annealing conditions and predict stability.

ACKNOWLEDGMENTS

The authors are grateful to Dane O. Kildsig Center for Pharmaceutical Processing Research (CPPR) for financial support. The authors would like to thank Dr. S. Yoshioka for the facilitation of the NMR work, and Dr. S. Tchessalov for experimental assistance and discussions. Also we acknowledge the support of the National Institute of Standards and Technology, U.S. Department of Commerce, in providing the neutron research facilities used in this work. This work utilized facilities supported in part by the National Science Foundation under Agreement No. DMR-0454672.

REFERENCES

1. Carpenter JF, Pikal MJ, Chang BS, Randolph TW. 1997. Rational design of stable lyophilized protein formulations: Some practical advice. Pharm Res 14:969–975.
2. Costantino HR. 2004. Excipients for use in lyophilized pharmaceutical peptide, protein, and other bioproducts. In: Costantino HR, Pikal MJ, editors. Lyophilization of biopharmaceuticals. edition. Arlington, VA: AAPS Press. pp. 139–228.
3. Pikal MJ. 1990. Freeze-drying of proteins. Part II: Formulation selection. BioPharm (Duluth, MN, United States) 3:26–30.
4. Pikal MJ. 1990. Freeze-drying of proteins. Part I: Process design. BioPharm (Duluth, MN, United States) 3:18–27.
5. Hill SA, Macnaughtan W, Farhat IA, Noel TR, Parker R, Ring G, Whitcombe MJ. 2005. The effect of thermal history on the Maillard reaction in a glassy matrix. J Agric Food Chem 53:10213–10218.
6. Abdul-Fattah AM, Truong-Le V, Yee L, Nguyen L, Kalonia DS, Cicerone MT, Pikal MJ. 2007. Drying-induced variations in physico-chemical properties of amorphous pharmaceuticals and their impact on

stability (I): Stability of a monoclonal antibody. J Pharm Sci 96:1983–2008.
7. Abdul-Fattah AM, Kalonia DS, Pikal MJ. 2007. The challenge of drying method selection for protein pharmaceuticals: Product quality implications. J Pharm Sci 96:1886–1916.
8. Sartor G, Mayer E, Johari G. 1994. Thermal history and enthalpy relaxation of an interpenetrating network polymer with exceptionally broad relaxation time distribution. J Polym Sci B Polym Phys 32: 683–689.
9. Abdul-Fattah Ahmad M, Truong-Le V, Yee L, Pan E, Ao Y, Kalonia Devendra S, Pikal Michael J. 2007 Drying-induced variations in physico-chemical properties of amorphous pharmaceuticals and their impact on stability. II: Stability of a vaccine. Pharm Res 24:715–727.
10. Franks F, Hatley RHM, Mathias SF. 1991. Materials science and the production of shelf-stable biologicals. BioPharm 4:38–42.
11 Mas Y-F, Prestrelski S. 2000. Biopharmaceutical powders: Particle formation and formulation considerations. Curr Pharm Biotechnol 1:283–302.
12. Pikal MJ. 2004. Mechanisms of protein stabilization during freeze-drying and storage: The relative importance of thermodynamic stabilization and glassy state relaxation dynamics. Drugs Pharm Sci 137:65–107.
13. Yoshioka S, Aso Y. 2007 Correlations between molecular mobility and chemical stability during storage of amorphous pharmaceuticals. J Pharm Sci 96:960–981.
14. Wang W. 2000. Lyophilization and development of solid protein pharmaceuticals. Int J Pharm 203: 1–60.
15. Pikal MJ. 2002. Chemistry in solid amorphous matrices: Implication for biostabilization. In: Levine H, editor. Amorphous food and pharmaceutical systems. edition. Cambridge, UK: The Royal Society of Chemistry. pp. 257–277.
16 Guo Y, Byrn SR, Zografi G. 2000. Physical characteristics and chemical degradation of amorphous quinapril hydrochloride. J Pharm Sci 89:128 143
17. Duddu SP, Zhang G, Dal Monte PR. 1997. The relationship between protein aggregation and molecular mobility below the glass transition temperature of lyophilized formulations containing a monoclonal antibody. Pharm Res 14:596–600.
18. Shamblin SL, Hancock BC, Pikal MJ 2006. Coupling between chemical reactivity and structural relaxation in pharmaceutical glasses. Pharm Res 23:2254–2263.
19. Pikal MJ, Rigsbee D, Roy ML, Galreath D, Kovach KJ, Wang B, Carpenter JF, Cicerone MT. 2008. Solid state chemistry of proteins: II. The correlation of storage stability of freeze-dried human growth hormone (hGH) with structure and dynamics in the glassy solid. J Pharm Sci 97:5206–5121.
20. Yoshioka S, Aso Y. 2005. A quantitative assessment of the significance of molecular mobility as a determinant for the stability of lyophilized insulin formulations. Pharm Res 22:1358–1364.
21. Yoshioka S, Aso Y, Miyazaki T. 2006. Negligible contribution of molecular mobility to the degradation rate of insulin lyophilized with poly(vinylpyrrolidone). J Pharm Sci 95:989–949.
22. Struik LCE. 1978. Physical aging in amorphous polymers and other materials. edition. New York, NY: Elsevier. p. 230.
23. Hodge IM. 1994. Enthalpy relaxation and recovery in amorphous materials. J Non-Crystal Solids 169: 211–266.
24. Pikal MJ. 1996. Thermometric seminars on calorimetry in materials sciences, Stockholm, Sweden.
25. Abdul-Fattah AM, Dellerman KM, Bogner RH, Pikal MJ. 2007. The effect of annealing on the stability of amorphous solids: Chemical stability of freeze-dried moxalactam. J Pharm Sci 96:1237–1250.
26. Luthra SA, Hodge IM, Utz M, Pikal MJ. 2008. Correlation of annealing with chemical stability in lyophilized pharmaceutical glasses. J Pharm Sci 97:5240–5251.
27. Wang B, Pikal MJ. The impact of thermal treatment on the stability of freeze dried amorphous pharmaceuticals: I. Dimer formation in sodium ethacrynate. J Pharm Sci: In press.
28. Carpenter JF, Prestrelski SJ, Anchordoguy TJ, Arakawa T. 1994. Interactions of stabilizers with proteins during freezing and drying. ACS Symposium Series (Formulation and Delivery of Proteins and Peptides), Vol. 567, pp. 134–147.
29. Chang L, Shepherd D, Sun J, Ouellette D, Grant KL, Tang X, Pikal MJ. 2005. Mechanism of protein stabilization by sugars during freeze-drying and storage: Native structure preservation, specific interaction, and/or immobilization in a glassy matrix? J Pharm Sci 94:1427–1444.
30. Shamblin SL, Zografi G. 1998. Enthalpy relaxation in binary amorphous mixtures containing sucrose. Pharm Res 15:1828–1834.
31. Liu J, Rigsbee DR, Stotz C, Pikal MJ 2002. Dynamics of pharmaceutical amorphous solids: The study of enthalpy relaxation by isothermal microcalorimetry. J Pharm Sci 91:1853–1862.
32. Pikal MJ, Chang L, Tang X. 2004. Evaluation of glassy-state dynamics from the width of the glass transition: Results from theoretical simulation of differential scanning calorimetry and comparisons with experiment. J Pharm Sci 93:981–994.
33. Kawakami K, Pikal MJ. 2005. Calorimetric investigation of the structural relaxation of amorphous materials: Evaluating validity of the methodologies. J Pharm Sci 94:948–965.

34. Prestrelski SJ, Pikal KA, Arakawa T. 1995. Optimization of lyophilization conditions for recombinant human interleukin-2 by dried-state conformational analysis using Fourier-transform infrared spectroscopy. Pharm Res 12:1250–1259.
35. Carpenter JF, Prestrelski SJ, Dong A. 1998. Application of infrared spectroscopy to development of stable lyophilized protein formulations. Eur J Pharm Biopharm 45:231–238.
36. Cicerone MT, Soles CL. 2004. Fast dynamics and stabilization of proteins: Binary glasses of trehalose and glycerol. Biophys J 86:3836–3845.
37. Cicerone MT, Soles CL, Chowdhuri Z, Pikal MJ, Chang L. 2005. Fast dynamics as a diagnostic for excipients in preservation of dried proteins. Am Pharm Rev 8:22, 24–27.
38. Roe RJ. 2000. Methods of X-Ray and neutron scattering in polymer science. New York: Oxford University Press. p. 352.
39. Wang B, Tchessalov S, Cicerone MT, Warne N, Pikal MJ. 2009. Impact of sucrose level on storage stability of proteins in freeze-dried solids: II. Correlation of aggregation rate with protein structure and molecular mobility. J Pharm Sci 98:3145–3168.
40. Yoshioka S, Miyazaki T, Aso Y, Kawanishi T. 2007. Significance of local mobility in aggregation of beta-galactosidase lyophilized with trehalose, sucrose or stachyose. Pharm Res 24:1660–1667.
41. Luthra SA, Uhz M, Pikal MJ. 2008. Solid state 13C NMR investigation of impact of annealing in lyophilized glasses. J Pharm Sci 97:4385–4846.
42. Webb SD, Cleland JL, Carpenter JF, Randolph TW. 2003. Effects of annealing lyophilized and spray-lyophilized formulations of recombinant human interferon-γ. J Pharm Sci 92:715–720.
43. Surana R, Pyne A, Suryanarayanan R. 2004. Effect of aging on the physical properties of amorphous trehalose. Pharm Res 21:867–874.
44. Earle JP, Bennett PS, Larson KA, Shaw R. 1991. The effects of stopper drying on moisture levels of Haemophilus influenzae conjugate vaccine. Dev Biol Stand 74:203–210.
45. Donovan PD, Cervuri V, Burton MD, Rajagopalan N. 2007. Effect of stopper processing conditions on moisture content and ramifications for lyophilized products: Comparison of "low" and "high" moisture uptake stoppers. PDA J Pharm Sci Technol 61:51–63.
46. Pikal MJ, Shah S. 1992. Moisture transfer from stopper to product and resulting stability implications. Dev Biol Stand 74:165–179.
47. Chang L, Shepherd D, Sun J, Tang X, Pikal MJ. 2005. Effect of sorbitol and residual moisture on the stability of lyophilized antibodies: Implications for the mechanism of protein stabilization in the solid state. J Pharm Sci 94:1445–1455.
48. Luthra SA, Hodge IM, Pikal MJ. 2008. Effects of annealing on enthalpy relaxation in lyophilized disaccharide formulations: Mathematical modeling of DSC curves. J Pharm Sci 97:3084–3099.
49. Shultz A, Young A. 1980. DSC on freeze-dried poly(methyl methacrylate)-polystyrene blends. Macromolecules 13:663–668.
50. Pikal MJ, Rigsbee DR, Roy ML. 2007. Solid state chemistry of proteins: I. Glass transition behavior in freeze dried disaccharide formulations of human growth hormone (hGH). J Pharm Sci 96:2768–2776.
51. Sarter G, Johari G. 1994. Calorimetric studies of the kinetic unfreezing of molecular motions in hydrated lysozyme, hemoglobin, and myoglobin. Biophys J 66:249–258.
52. Borde B, Bizot H, Vigier G, Buleon A. 2002. Calorimetric analysis of the structural relaxation in partially hydrated amorphous polysaccharides. II. Phenomenological study of physical ageing. Carbohydr Polym 48:111–123.
53. Vyazovkin S, Dranca I. 2006. Probing beta relaxation in pharmaceutically relevant glasses by using DSC. Pharm Res 23:422–428.
54. Gunawan L, Johari G, Shanker R. 2008. Structural relaxation of acetaminophen glass. Pharm Res 23: 967–979.
55. Pikal MJ, Rigsbee D, Roy MJ. 2008. Solid state stability of proteins III: Calorimetric (DSC) and spectroscopic (FTIR) characterization of thermal denaturation in freeze dried human growth hormone (hGH). J Pharm Sci 97:5122–5131.
56. Lunkenheimer P, Wehn R, Schneider U, Loidl A. 2005. Glassy aging dynamics. Phys Rev Lett 95:1–4.
57. Nagai K, Freeman BD, Watanabe T, Nakagawa T. 1999. Effects of physical aging on gas permeability and molecular motion in poly(1-trimethylsilyl-1-propyne). ACS Symposium Series, Vol. 733, pp. 95–101.
58. Smits ALM, Ruhnau FC, Vliegenthart JFG, Van Soest JJG. 1998. Aging of starch based systems as observed with FT-IR and solid state NMR spectroscopy. Starch/Stärke 50:478–483.
59. Etienne S, Hong N, Duval E, Mermet A, Wypych A, David L. 2007. Physical aging and molecular mobility of amorphous polymers. J Non-Cryst Solids 353:3871–3878.
60. Perez J, Cavaille JY, David L. 1999. New experimental features and revisiting the alpha and beta mechanical relaxation in glasses and glass-forming liquids. J Mol Struct 479:183–194.
61. Perez J, Cavaille J Y, Diaz Calleja R, Gomez Ribelles JL, Monleon Pradas M, Ribes Greus A. 1991. Physical aging of amorphous polymers. Theoretical analysis and experiments on poly(methyl methacrylate). Makromol Chem 192:2141–2161.
62. Muzeau E, Vigier G, Vassoille R. 1994. Physical aging phenomena in an amorphous polymer at temperatures far below the glass transition. J Non-Cryst Solids 172–174:575–579.

63. Muzeau B, Vigier G, Vassoille R, Perez J. 1995. Changes of thermodynamic and dynamic-mechanical properties of polymethyl methacrylate due to structural relaxation-low-temperature aging and modeling. Polymer 36:615–620.
64. Hill JJ, Shalaev EY, Zografi G. 2005. Thermodynamic and dynamic factors involved in the stability of native protein structure in amorphous solids in relation to levels of hydration. J Pharm Sci 94:1633–1667.
65. Bhugra C, Shmeis R, Krill SL, Pikal MJ. 2008. Predictions of onset of crystallization from experimental relaxation times. I—Correlation of molecular mobility from temperatures above the glass transition to temperatures below the glass transition. Pharm Res 25:2271–2290.

Feasibility of ^{19}F-NMR for Assessing the Molecular Mobility of Flufenamic Acid in Solid Dispersions

Yukio Aso,* Sumie Yoshioka, Tamaki Miyazaki, and Toru Kawanishi

National Institute of Health Sciences; 1–18–1 Kamiyoga, Setagaya, Tokyo 158–8501, Japan.
Received September 9, 2008; accepted October 22, 2008; published online October 23, 2008

The purpose of the present study was to clarify the feasibility of ^{19}F-NMR for assessing the molecular mobility of flufenamic acid (FLF) in solid dispersions. Amorphous solid dispersions of FLF containing poly(vinylpyrrolidone) (PVP) or hydroxypropylmethylcellulose (HPMC) were prepared by melting and rapid cooling. Spin–lattice relaxation times (T_1 and $T_{1\rho}$) of FLF fluorine atoms in the solid dispersions were determined at various temperatures (−20 to 150 °C). Correlation time (τ_c), which is a measure of rotational molecular mobility, was calculated from the observed T_1 or $T_{1\rho}$ value and that of the T_1 or $T_{1\rho}$ minimum, assuming that the relaxation mechanism of spin–lattice relaxation of FLF fluorine atoms does not change with temperature. The τ_c value for solid dispersions containing 20% PVP was 2—3 times longer than that for solid dispersions containing 20% HPMC at 50 °C, indicating that the molecular mobility of FLF in solid dispersions containing 20% PVP was lower than that in solid dispersions containing 20% HPMC. The amount of amorphous FLF remaining in the solid dispersions stored at 60 °C was successfully estimated by analyzing the solid echo signals of FLF fluorine atoms, and it was possible to follow the overall crystallization of amorphous FLF in the solid dispersions. The solid dispersion containing 20% PVP was more stable than that containing 20% HPMC. The difference in stability between solid dispersions containing PVP and HPMC is considered due to the difference in molecular mobility as determined by τ_c. The molecular mobility determined by ^{19}F-NMR seems to be a useful measure for assessing the stability of drugs containing fluorine atoms in amorphous solid dispersions.

Key words ^{19}F-NMR; molecular mobility; stability; crystallization; solid dispersion

Amorphous solid dispersions are used for improving the dissolution rate and solubility of poorly soluble drugs. However, drugs in amorphous form are generally less stable than crystalline drugs because of their higher energy state and higher molecular mobility. It is well known that polymeric excipients can reduce the crystallization rate of many amorphous drugs.[1—12] This stabilization by poly(vinylpyrrolidone) (PVP) is partly attributable to its ability to decrease molecular mobility, as indicated by increases in the glass transition temperature (T_g).[9] Therefore, it is of great interest to estimate the molecular mobility of drugs in solid dispersions. Although ^{13}C-NMR relaxation measurements are useful for assessing the molecular mobility of drugs in solid dispersions,[13] the low sensitivity of ^{13}C because of its low natural abundance is a drawback of ^{13}C-NMR. In contrast to ^{13}C, ^{19}F has very favorable sensitivity in NMR experiments, since it is present in 100% natural abundance, is second only to the proton in its resonance frequency (except ^{3}H) and has a spin quantum number of 1/2. The receptivity for ^{19}F is 83% of that for ^{1}H and 4700 times of that for ^{13}C.[14] Many drugs containing fluorine atoms are listed in The Japanese Pharmacopoeia. In contrast, almost all pharmaceutical excipients do not contain fluorine atoms. ^{19}F-NMR may therefore have an advantage over ^{13}C-NMR or ^{1}H-NMR for selectivity and sensitivity when assessing the molecular mobility of drugs containing fluorine atoms in pharmaceutical dosage forms such as solid dispersions.

The orientations and molecular mobility of flufenamic acid (FLF)[15] and ^{19}F-labeled α-tocopherol[16] in a lipid bilayer were studied using ^{19}F-NMR. Structures and molecular mobility of ^{19}F-labeled peptides and proteins in biological membranes were also investigated.[17—20] To the authors' knowledge, application of ^{19}F-NMR to studies of drug molecular mobility in solid dispersions has not been reported. This paper describes the feasibility of ^{19}F-NMR for assessing the molecular mobility of FLF in PVP or hydroxypropylmethylcellulose (HPMC) solid dispersions, and discusses the effect of polymer excipients on the crystallization tendency of FLF in solid dispersions in terms of differences in molecular mobility.

Experimental

Materials FLF (Fig. 1) was purchased from Wako Pure Chemical Industry (Osaka), and PVP and HPMC were from Sigma (St. Louis, MO, U.S.A.). FLF solid dispersions with PVP or HPMC were prepared by melting and cooling of mixtures of FLF with PVP or HPMC. The solid dispersions obtained were confirmed to be amorphous from microscopic observation under polarized light.

Nuclear Magnetic Relaxation Measurements ^{19}F-NMR measurements were carried out using a model JNM-MU25 pulsed NMR spectrometer (JEOL DATUM, Tokyo) operating at a resonance frequency of 25 MHz. Time profiles of spin–spin relaxation of the ^{19}F atoms of FLF were measured using the "solid echo" pulse sequence to overcome the dead time of the instrument. Spin–lattice relaxation time in the laboratory frame (T_1) was measured using the inversion recovery pulse sequence. Spin–lattice relaxation time in the rotating flame ($T_{1\rho}$) was measured at spin locking intensity of 10 G.

DSC Measurements T_g of FLF-PVP and FLF-HPMC solid dispersions was measured by DSC using a model 2920 differential scanning calorimeter and a refrigerator cooling system (TA Instruments, Newcastle, DE, U.S.A.). Approximately 5 mg of each solid dispersions was put into an aluminum sample pan and then sealed hermetically. T_g was measured at a heating rate of 20 °C/min. Temperature calibration of the instrument was carried out using indium.

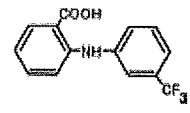

Fig. 1. Structure of FLF

* To whom correspondence should be addressed. e-mail: aso@nihs.go.jp

Results and Discussion

Molecular Mobility of FLF as Measured by ^{19}F-NMR Spin–Lattice Relaxation Time T_1 and $T_{1\rho}$ of fluorine atoms of FLF in PVP and HPMC solid dispersions were measured using a pulsed NMR spectrometer in the temperature range from −20 to 150 °C. T_1 is sensitive to the molecular motion on the time scale of the resonance frequency (MHz order). On the other hand, $T_{1\rho}$ is sensitive to the molecular motion with a frequency equivalent to the intensity of spin locking field (typically mid kHz order).[21] The temperature dependence of T_1 and $T_{1\rho}$ exhibits minimum at a specific temperature at which the molecules of interest have molecular motion with MHz time scale or mid kHz time scale predominantly. The resonance frequency of 25 MHz, lower than that of a conventional high resolution NMR spectrometer, was used to observe T_1 minimum in the temperature rage studied. Figure 2 shows the temperature dependence of T_1 and $T_{1\rho}$ of FLF fluorine atoms in PVP and HPMC solid dispersions. For FLF–PVP solid dispersions (7 : 3), the minimum of T_1 or $T_{1\rho}$ was observed at about 90 °C and 60 °C, respectively (Fig. 2A). When the PVP content decreased to 20% (w/w), T_1 and $T_{1\rho}$ of FLF at temperatures above 70 °C could not be determined due to rapid crystallization. Similar temperature dependence of T_1 or $T_{1\rho}$ was observed for the FLF–HPMC solid dispersions (Fig. 2B). The temperature difference between T_1 and $T_{1\rho}$ minimum is considered to be due to the difference in the time scale of molecular motion reflected on T_1 (MHz order) and $T_{1\rho}$ (mid kHz order). Since the molecular motion on MHz time scale becomes predominant at higher temperature than molecular motion on mid kHz time scale, T_1 minimum is observed at higher temperature than $T_{1\rho}$ minimum.

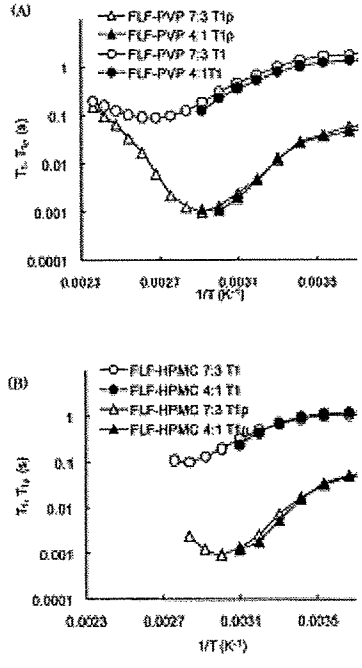

Fig. 2. Temperature Dependence of T_1 and $T_{1\rho}$ of FLF Fluorine Atoms in PVP (A) and HPMC (B) Solid Dispersions

We made following assumptions in order to estimate the molecular mobility of FLF from T_1 and $T_{1\rho}$ of FLF fluorine atoms: first, we assumed that FLF fluorine atoms in the solid dispersions relaxes mainly *via* dipolar interaction, and that the contribution of the spin–rotation interaction mechanism[21] is negligible. While relaxation *via* the spin–rotation interaction mechanism has been reported for liquid sample,[22–24] complete domination of dipolar interactions has been reported for fluorine atoms for polycrystalline van der Waals molecular solid.[25] We also made an assumption that the contribution of the cross-relaxation between fluorine and proton atoms can be considered small. It is known that relaxation is not intrinsically single-exponential when cross-relaxation between fluorine and proton atoms takes place.[14] However, we assumed small contribution of the cross-relaxation, because the relaxation of FLF fluorine atoms in the solid dispersions was exponential within experimental uncertainty. In studies of molecular motions, a large number of models describing molecular motions have been proposed for calculation of the spectrum density function.[26] We used a simple model that the molecular motion reflected on T_1 or $T_{1\rho}$ is represented by single correlation time for the purpose of comparing the mobility of FLF in the PVP and HPMC solid dispersions. According to the above assumptions, T_1 and $T_{1\rho}$ are described by Eqs. 1 and 2.[21]

$$\frac{1}{T_1} = \frac{6}{20}\frac{\gamma^4\hbar^2}{r^6}\left\{\frac{\tau_c}{1+\omega_0^2\tau_c^2}+\frac{4\tau_c}{1+4\omega_0^2\tau_c^2}\right\} \quad (1)$$

$$\frac{1}{T_{1\rho}} = \frac{3}{20}\frac{\gamma^4\hbar^2}{r^6}\left\{\frac{3\tau_c}{1+4\omega_1^2\tau_c^2}+\frac{5\tau_c}{1+\omega_0^2\tau_c^2}+\frac{2\tau_c}{1+4\omega_0^2\tau_c^2}\right\} \quad (2)$$

where τ_c is the correlation time that characterizes molecular reorientations, and ω_0 and ω_1 are the resonance frequencies of fluorine atoms in the static magnetic field and spin locking field, respectively. γ, r and $\hbar$ are the gyromagnetic ratio of fluorine, the distance of neighboring fluorine atoms, and the Plank constant divided by 2π, respectively. Equations 1 and 2 infer that T_1 and $T_{1\rho}$ become minimal when $\omega_0\tau_c$ is approximately 0.62[27] and $\omega_1\tau_c$ is approximately 0.52,[21] respectively. When the minimum of T_1 or $T_{1\rho}$ is observed, we can calculate the unknown value, r, in Eqs. 1 and 2. If r is known, the τ_c value can be calculated from the observed T_1 or $T_{1\rho}$ value, assuming that r does not change with temperature.

The values of r calculated from the T_1 and $T_{1\rho}$ minimum observed for the FLF–PVP solid dispersion (7 : 3) were 2.3 and 2.4 Å, respectively, and similar r values were obtained for the FLF–HPMC solid dispersion (7 : 3). These values are comparable to the reported value (2.174 Å) for 3-(trifluoromethyl)phenanthrene,[25] indicating that dipole interaction between neighboring fluorine atoms can be considered the predominant relaxation mechanism of FLF fluorine atoms in the solid dispersions. The difference between the r values obtained in this work and the reported value suggests that the possibility of the spin–rotation interaction mechanism and/or dipole interaction between fluorine and proton atoms cannot be excluded as a relaxation mechanism of FLF fluorine atoms.

Figure 3 shows the temperature dependence of τ_c calculated from T_1 and $T_{1\rho}$ for FLF fluorine atoms in the solid dis-

persions. The τ_c of FLF fluorine atoms in PVP solid dispersions calculated from $T_{1\rho}$ was 8.2 μs at 50 °C, which was about 3 times larger than that in HPMC solid dispersions (2.6 μs), indicating that the molecular mobility of FLF was lowered more strongly by PVP than by HPMC.

The τ_c values calculated using T_1 values differ from those calculated from $T_{1\rho}$ values. The slope of temperature dependence of τ_c changed around T_g. These findings suggest that the assumption that the molecular motion reflected on T_1 and $T_{1\rho}$ is represented by a single τ_c may be too simple to describe the molecular motion of FLF in the solid dispersions at temperatures studied, and that two or more molecular motions, such as rotation of trifluoromethyl group and motions with larger scales than rotation of trifluoromethyl group, may be reflected on T_1 and $T_{1\rho}$. Further studies including ^{1}H-NMR relaxation measurement and dielectric relaxation measurements will be needed to identify the detailed molecular motion of FLF in the solid dispersions.

Correlation between Crystallization Tendency and Molecular Mobility of FLF in Solid Dispersions Crystallization proceeds *via* formation of crystal nuclei and crystal growth. As a measure of the crystallization tendency of amorphous FLF in solid dispersions, the overall crystallization rate of amorphous FLF in the solid dispersions was estimated from the time profiles amorphous FLF remaining in the solid dispersions instead of measuring the nucleation rate and growth rate. Amorphous FLF remaining in the solid dispersions was estimated by analyzing solid echo signals of FLF fluorine atoms. Figure 4 shows the solid echo signal of fluorine atoms of FLF in solid dispersions containing 20% (w/w) PVP and that of fluorine atoms of crystalline FLF. The signal for the solid dispersions was describable by the Lorentzian relaxation equation (Eq. 3), and its relaxation time (T_{2L}) was approximately 140 μs. Crystalline FLF exhibited Gaussian relaxation signals (Eq. 4), and its relaxation time (T_{2G}) was approximately 30 μs. These results indicate that amorphous FLF in solid dispersions is considered to exhibit Lorentzian relaxation signals.

$$I = I_0 \exp(-t/T_{2L}) \tag{3}$$

$$I = I_0 \exp\{-t^2/(2T_{2G}^2)\} \tag{4}$$

where I_0 and I represent the signal intensities at time 0 and t, respectively. Figure 5 shows solid echo signals for the fluorine atoms of FLF in the solid dispersions stored at 60 °C. Samples stored at 60 °C exhibited biphasic decay signals, and signals were describable by summation of the Gaussian (solid line) and Lorentzian (dashed line) equations (Eq. 5).

$$I = I_0\{P_L \exp(-t/T_{2L}) + P_G \exp(-t^2/2T_{2G}^2)\} \tag{5}$$

where P_L and P_G are the ratio of fluorine atoms exhibiting Lorentzian and Gaussian relaxation process, respectively, and $P_L + P_G = 1$. Assuming that the T_{2L} and T_{2G} values are 140 and 30 μs, respectively, P_L values of FLF in the solid dispersions were estimated by curve fitting. P_L values of the solid dispersions decreased with increasing storage time, indicating that crystallization of amorphous FLF in solid dispersions takes place during storage at 60 °C. To certify the reliability of the P_L values obtained by ^{19}F-NMR measurements, change in the heat capacity at T_g ($\Delta C_p(T_g)$) was determined for the solid dispersions stored at 60 °C for various periods as a measure of amorphous FLF remaining, and was compared with the value of P_L. As shown in Fig. 6, the P_L value was proportional to the $\Delta C_p(T_g)$ value, and was considered to be a useful measure of amorphous FLF remaining in the solid dispersions.

Figure 7 shows the time profiles of the P_L values for FLF solid dispersions containing 20% (w/w) PVP or HPMC at 60 °C. The decrease in the ratio of Lorentzian fluorine atoms was faster for HPMC solid dispersions than for PVP solid dispersions, indicating that the overall crystallization rate of FLF in HPMC solid dispersions is larger than that in PVP solid dispersions. The overall crystallization rate depends on both molecular mobility (the rate of diffusion across the interface between crystalline and amorphous phase) and ther-

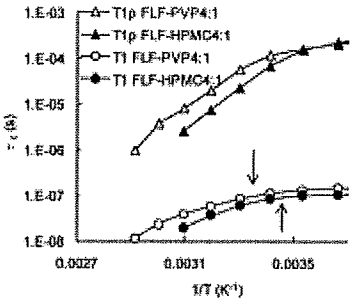

Fig. 3. Temperature Dependence of τ_c of FLF Fluorine Atoms in PVP and HPMC Solid Dispersions

Arrows in the figure represent T_g.

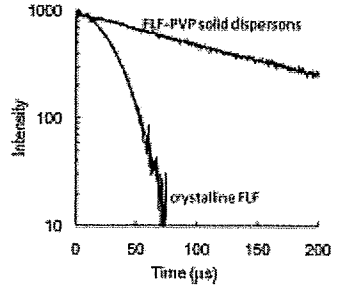

Fig. 4. Typical Solid Echo Signal of Fluorine Atoms of FLF in the Freshly Prepared Solid Dispersion Containing 20% (w/w) PVP and That of Fluorine Atoms of Crystalline FLF

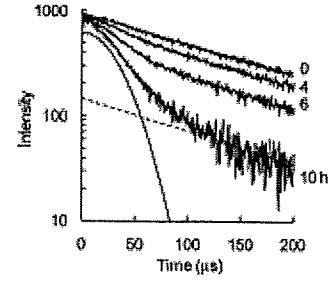

Fig. 5. Typical Solid Echo Signals of Fluorine Atoms of FLF in the Solid Dispersions Containing 20% (w/w) PVP Stored at 60 °C